Peak Discharge Determination using HEC-HMS for Flood Analysis: A Case of San Simon, Pampanga

Francine Kaye O. Tolentino [1], Allan Paul B. David [1], Karla Sue D. Galang [1], Eriane O. Laxamana [1], Mark Louis L. Pangilinan [1], Euvilaine R. Ranara [1], Aaron S. Malonzo [2], John Vincent G. Tongol [2]

[1]*Student, Department of Civil Engineering, College of Engineering and Architecture, Don Honorio Ventura State University, Bacolor, Pampanga, Philippines.*

[2]*Faculty, Department of Civil Engineering, College of Engineering and Architecture, Don Honorio Ventura State University, Bacolor, Pampanga, Philippines.*

Corresponding Author: francinekayeotolentino@gmail.com

Abstract: - In order to address problems regarding flooding, modeling is now widely recognized as an effective tool for dealing with the complex dynamics, large-scale, and unpredictability of water resource systems. Hydrological modeling, in particular, is a frequently used method for estimating a basin's hydrological response to precipitation. This study was conducted in San Simon, Pampanga. It is one of the flood-prone areas in the province of Pampanga. It is a town that sits along the Pampanga River basin. This study was able to determine the peak discharges of the subbasins enclosed by the boundary of San Simon. This study utilized the QGIS software to delineate each subbasin as well as HEC-HMS software to generate the discharge hydrograph and determine the peak discharges of each subbasin based on design storm with 2-, 5-, 10-, 15-, 20-, 25-, 50- and 100-year return period. Moreover, the maximum capacity of the subbasins were computed manually and were compared to the simulated peak discharges to determine if there is flooding or not. The highest peak discharge for all elements was calculated for the 100-year return period design storm while the lowest was calculated on the 2-year return period. Some parts were already flooded in Subbasin 6 by the design storm with a 10-year return period. For the succeeding year return periods, namely 10-, 15-, 20-, 25-, 50- and 100-year return periods, selected stations from Subbasin, 4,5 and 6 were all flooded. The simulation of peak discharge data generated in this study can be utilized for flood management. Moreover, the data generated from this study can also be used to lower the danger of flooding through hydraulic modeling and mapping the flood inundation zones.

Key Words: — ***Flooding, Hydrologic Modelling, Year Return Periods, Peak Discharge, Discharge Hydrograph, HEC-HMS.***

I. INTRODUCTION

Philippines is known for being prone to various disasters or extreme events brought about by weather conditions. Geophysical disasters, and disasters related to the climate are common occurrences in the nation.

Manuscript revised June 19, 2023; accepted June 20, 2023. Date of publication June 25, 2023.

This paper available online at www.ijprse.com

ISSN (Online): 2582-7898; SJIF: 5.59

According to the report by Bricker et al (2014), the Philippines frequently encounters rain-bearing winds and significant levels of precipitation because of its tropical location. The country experiences 20 typhoons on average each year.

Flooding is recognized as one of the most catastrophic natural disasters, inflicting disastrous and costly damage to human lives, infrastructure, and the environment all over the world (Santillan et al., 2016). Flooding, defined as the rising and overflowing of a body of water, particularly into typically dry ground, is one of the many catastrophic natural events. River flooding happens when a significant amount of rain falls in a river system with tributaries draining large areas with many independent river basins, inundating the neighboring low-lying areas. This occurs when the volume of water in a river exceeds

its ability to hold it (Sulistyowati et al., 2016). The Philippines' vulnerability to river flooding is noticeable because of the archipelago's 421 major river basins (Callanga et al., 2020).

Understanding floods and assessing the risks associated with them, including the development of warning systems and forecasting, as well as the planning and implementation of flood adaptation and mitigation measures, have become more crucial in modern society as floods are the most common natural disaster that affects more people globally than any other natural disaster (Santillan et al., 2016). Flood simulation, modeling, and mapping are some of the most well-known methods for assessing flood risk and vulnerability (Puno et al., 2018). Moreover, to warn the public of the potential impending flood calamity, an accurate and reliable prediction model of the individual rivers that cause flooding in highly populated areas is required (Adnan et al., 2016). Modeling has been used for a variety of purposes, including (1) general evaluation of condition as well as performance of water resource systems and studying its behavior; (2) evaluating possible solutions to restore, enhance, preserve, and/or manage both the amount and the quality of the water resource system; (3) developing operational guidelines to ensure sufficient water quantity with desirable water quality; and (4) inspection, detection, and monitoring (5) real-time water quantity and quality forecasting; (6) water resource system operation forecasting for possible future situations (Tabios III, G. Q., 2020).

In the most advanced hydrologic field, flood models and mathematical methods are becoming increasingly essential topics, notably to simulate river water level and streamflow to anticipate floods (Faruq, 2021). Furthermore, river flood modeling is a method used to assess, analyze, and foresee the risk of flood caused by the river in a variety of scenarios. The four main components of river flood risk modeling are hydrological modeling, hydraulic modeling, river flood visual analytics, and river flood risk mapping (Alaghmand et al., 2012). A precise description of the parameters as well as a suitable representation of the channel of the river and floodplain geometry are necessary for a river flood model to be accurate and effective in predicting the flow volume and water levels along the reach (Gichamo et al., 2012).

Severe flooding is a typical occurrence in the Pampanga River basin. It is the second largest river basin on the island of Luzon. Increasingly frequent direct tropical typhoon strikes and intensified monsoon rainfall have both put the basin in danger (Nagumo & Sawano, 2016).

Additionally, San Simon is a town that sits along the Pampanga River basin. San Simon is a flat, low-lying municipality made up of 14 barangays (the smallest administrative unit in the Philippines), six of which are prone to floods due to their proximity to the Pampanga River (Barnes et al., 2020). Hydrological models and studies regarding the subbasins enclosed by the boundary of San Simon will be very helpful to robust understanding regarding the flooding that happens in the municipality.

1.1 Background of the Study

Natural calamities such as landslides, tropical cyclones, earthquakes, and most especially, typhoons are common to the Philippines, particularly from Typhoon "Pablo" in 2012, Super Typhoon "Yolanda" (international name: Haiyan) in 2013, and the onslaught of Typhoon "Ulysses" (international name: Vamco) in 2020. One of the effects of the precipitation brought by typhoons is flooding. Flooding is severe in areas near rivers due to rising river water levels and can endanger communities (M. S. H. Mondal et al. 2020). Modeling is a crucial tool for producing science-based information and is helpful for creating policies and management actions, and then for putting strategies and operational procedures into place for successful water resource planning, design, and management (Tabios III, G. Q., 2020). Specifically, hydrological modeling is a widely used approach for estimating the hydrological response of a basin to precipitation. The need for such a modeling system is prompted, and in some cases even enforced, by the numerous activities necessary for river basin management and preparation, such as immediate flood warnings and delineation of areas at risk of flooding, and the scheduling of the water budget at the scale of the basin in accordance with national and local guidelines in the field (Halwatura & Najim, 2013). This study created a hydrologic model of the subbasin enclosed by the boundary of San Simon, Pampanga. Moreover, it was able to determine the occurrence of flooding in some areas of San Simon by comparing the simulated peak discharges based on different design storms with the computed maximum capacity per cross section. The peak discharge determination, and flood identification and analysis done by the study can help provide substantial knowledge of the flooding that occurs in the municipality of San Simon, Pampanga.

1.2 Objectives of the Study

The objective of this research is to use the Hydrologic Modelling System (HEC-HMS) to create a hydrological model of subbasins along the boundary of San Simon, Pampanga and

perform flood analysis. The researchers identified the peak discharges of each subbasins and determined if there was an occurrence of flooding by comparing it with the computed maximum capacity of the cross section.

1.3 Significance of the Study

The data gathered from this study contributes in providing inputs for flood modeling and improving understanding of the floods that occur in the municipality of San Simon, Pampanga. Specifically, the study will be beneficial to the local government unit of San Simon, Pampanga, the residents and the future researchers.

1.4 Scope and Limitation

This study identified the subbasin inside San Simon, Pampanga and delineated the physical characteristics of the watershed. It created discharge hydrographs for the subbasins along the boundary of San Simon, Pampanga. It was able to simulate the peak discharges of each subbasins based on design storms with 2-, 5-, 10-, 15-, 20-, 25-, 50- and 100-year return periods through HEC-HMS. The maximum capacity per cross section was also computed manually using the cross-section generated in HEC-RAS. The simulated peak discharges were then compared to the maximum capacity per cross section to determine if there is flooding or not. The data and model generated from the study can be used for flood analysis and as inputs for hydraulic modeling.

One limitation of the study is that the RIDF data were acquired from only one RIDF station. Specifically, it was obtained from the station in Cansinala, Apalit which is the only RIDF station in Pampanga according to Hydrometeorological Data Applications Section, Hydro-Meteorology Division (HMDAS HMD), PAGASA. Moreover, due to challenges of the simulation in HEC-RAS, the visual representation of the flooding that happens in the community was not generated. The HEC-RAS software was only utilized in determining the cross section, its station and elevation. Manual computations and theoretical approaches were used instead to complete the flood analysis. Furthermore, due to lack of resources to obtain a more accurate DEM, the cross-sections presented were limited to those with well-defined cross sections and with areas that can be solved theoretically.

In addition, the researchers were unable to undertake site surveys and site validation due to the short time frame to conduct the study. Furthermore, the study was limited to the municipality of San Simon, Pampanga and the approach to the problem will not be structural.

1.5 Conceptual Framework

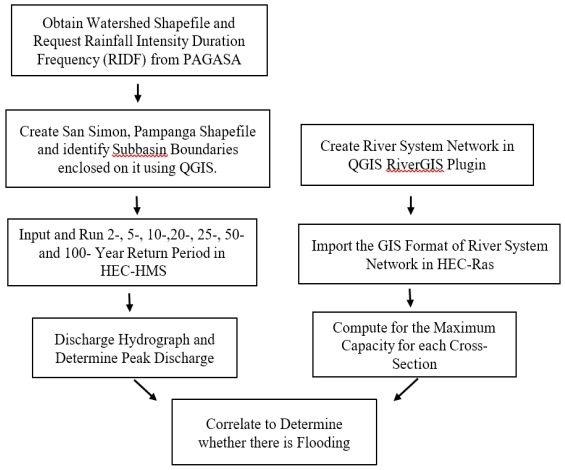

Fig.1. An illustration of the approach that has been done in the study.

II. METHODOLOGY

2.1 Methodological Framework

2.1.1 Research Design

Inductive reasoning was the method used in the research. It is an investigation to identify the peak discharge of each subbasin. The study is quantitative in nature. This method was used by researchers to examine theories based on statistical and mathematical evidence.

2.1.2 Research Instrument

QGIS software was utilized to define the catchments that are enclosed in the boundary of San Simon, Pampanga. QGIS is a free and open-source software application that allows users to generate, alter, browse, analyze, and publish spatial data.

Moreover, the hydrologic models were developed using HEC HMS. According to USACE HEC, the HEC HMS is a generic modeling system created to simulate the precipitation-runoff processes of watershed systems with a variety of applications, such as large river basin water supply and flood hydrology, as well as small urban or natural watershed runoff (Toda et al., 2017). The HEC-HMS model does not require river geometry data, the input data used is less complex when determining the flood discharge of a watershed.

The study also utilized Rainfall Intensity Duration Frequency (RIDF) data that were collected from the local station in

Cansinala, Apalit, Pampanga to create the model. Meanwhile, HEC-RAS was utilized to obtain the cross-section of the subbasin. HEC RAS is often used to calculate and examine the hydraulics of floodplain using an output hydrograph from the HEC HMS. Flood inundation mapping is one of the most popular applications for HEC RAS, assuming that inflow data is available to serve as the model's boundary conditions.

2.2 Data Collection

The Rainfall Intensity Duration Frequency (RIDF) data of the station in Cansinala, Apalit, Pampanga were gathered from Philippine Atmospheric, Geophysical and Astronomical Services Administration (PAGASA). The proponents obtained a delineated watershed shapefile which was used to identify the watersheds under the area of San Simon, Pampanga using QGIS. The Land Cover Map of Region 3 (year 2020) was acquired from geoportal PH and was processed in QGIS.

2.3 Data Analysis and Evaluation

2.3.1 Subbasin Boundaries preparation using QGIS and Watershed Delineation

There are 11 subbasins under the area of San Simon, Pampanga. The Subbasin boundaries were identified from the watershed shapefile gathered by the researchers. QGIS software was used to select the subbasins under the study area. Meanwhile, the basin model was made using HEC-HMS. The subbasin boundaries under the study area and the rivers that were identified by QGIS are shown in Figure 2.

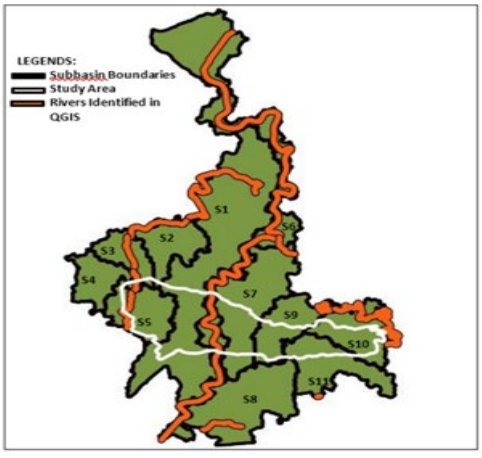

Fig.2. Subbasin Boundaries under the Study Area

2.3.2 Processing of Rainfall Intensity Duration Frequency (RIDF) data to create Discharge Hydrograph using HEC-HMS

The processed sub-basin model, Rainfall Intensity Duration Frequency (RIDF) data gathered from Philippine Atmospheric, Geophysical and Astronomical Services Administration (PAGASA) will be used as inputs to simulate and produce the discharge hydrograph from HEC HMS.

In this study, Soil Conservation Service (SCS) Curve Number (CN) method was utilized as loss method in HEC-HMS. SCS-CN method offers simplicity, predictability, and stability in estimating and predicting runoff (Balvanshi and Tiwari, 2019).

The SCS established an empirical relationship between Initial abstraction (Ia) and Potential Maximum Retention (S) through the examination of data from numerous small experimental watersheds as follows:

$$\boldsymbol{S = \frac{1000-10CN}{CN}\ (foot-pound\ system)}$$

$$\boldsymbol{S = \frac{25400-254CN}{CN}\ (SI)}$$

$$\boldsymbol{Ia = 0.2 * S}$$

where:

Ia = the initial abstraction (initial loss), in or mm

S = potential maximum retention, a measure of the ability of a watershed to abstract and retain storm precipitation, in or mm

CN = curve number

A composite CN is calculated as follows for a watershed made up of several soil types and land uses:

$$CN_{composite} = \frac{\sum A_i CN_i}{\sum A_i}$$

where:

$CN_{composite}$ = the composite CN used for runoff volume computations

i = an index of watershed subdivisions of uniform land use and soil type

CN_i = the CN for subdivision i

A_i = the drainage area of subdivision i

Moreover, Snyder unit hydrograph was used as the transformation method in the model. It requires the Standard Lag (HR) and peaking coefficient as inputs in HEC-HMS. The lag time parameter was computed using the formula:

$$t_l = C_t(LL_c)^{0.3}$$

where:

L = length of the main stream from the outlet to the divide (mi)
L_c = length along the main stream to a point nearest the watershed centroid (mi)

C_t = timing coefficient

Meanwhile, the routing method that was utilized in the study was lag routing. The lag routing method, which may be used within HEC-HMS, is the simplest hydrologic routing technique currently known. Lag routing was utilized in the study due to constraints in acquired data.

The Rainfall Intensity - Duration Frequency (RIDF) Analysis data of the station in Cansinala, Apalit was utilized in the study. Under the Meteorological Models Component of HEC-HMS, Frequency Storm was selected and the RIDF data were used as inputs.

A six-day simulation run with a start date of 03 May 2023 and an end date of 09 May 2023 was made for the Control Specifications. Both the beginning and the end times were set at 12:00 AM (00:00). Additionally, the model was given an hourly time interval.

Afterwards, the compute function was utilized in HEC HMS to get the results for the peak discharge of each element based on design storms with 2-, 5-, 10-, 15-, 20-, 25-, 50- and 100-year return.

2.3.3 Manual Maximum Capacity Computation

A HEC-RAS geometry file was made as the initial stage in constructing the HEC-RAS model. Inputting cross-section data, specifying all necessary junction data, including hydraulic structure data, pump stations, storage areas, and two-dimensional flow areas are all part of the geometric data (also known as the "River System Schematic"). Geometric data can be imported into HEC-RAS in a number of different formats. One of the formats is a GIS format (created at HEC). RiverGIS is a QGIS plugin for generating geometry models for HEC-RAS flow models from spatial data.

Figure 3 shows the river networks in subbasin 4, 5, and 6 along the study area. The elevation data used in processing the model was obtained from the Global Multi-resolution Terrain Elevation Data 2010 (GMTED2010) from the U.S. Geological Survey (USGS). The cross-section cut lines were picked from the available cut lines with cross sections that are well-defined and with areas that may be solved manually.

Fig.3. River Networks of Subbasins 4,5 and 6

In all hydraulic calculations relating to flow in open channels, an assessment of the channel's roughness characteristics is utilized. The appropriate Manning's coefficient's selection is crucial for the accuracy of simulated water surface profiles. (Hadi & Almansori, 2023). In selecting n value, Cowman (as cited in Garcia et al., 2015) provided a general equation for the Manning's Roughness Coefficient using the formula:

$$n = (n_0 + n_1 + n_2 + n_3 + n_4)m$$

where:
n_0 = n value for straight uniform and smooth channel
n_1 = correction for surface irregularities
n_2 = correction for shape variations
n_3 = correction for obstructions
n_4 = correct for vegetation
m = for degree of meandering

The Manning's Roughness Coefficient Values of the chosen station of Subbasin 4,5, and 6 are shown in the table below.

Table.1. Manning's Roughness Coefficient Value of Subbasin 4,5 and 6

Subbasin	Station	n
Subbasin-4	531.9539	0.061
Subbasin-5	1551.457	0.053
Subbasin-6	4285.935	0.048
	2120.811	0.0884
	916.8855	0.063

The area-velocity approach is the most often used flow measuring method in both shallow and deep rivers because it is an accurate method that is simple to utilize in the field. The product of area and velocity yields streamflow (Clasing & Muñoz, 2018).

It is represented by the formula:

$$Q = Av$$

Where Q denotes discharge (in cfs or cms); A is the cross-sectional area of the channel at a specific transect; and v denotes the mean water-column velocity at a certain transect.
Manning's equation is more frequently utilized to calculate discharge where bed roughness is an essential consideration. It is written as:

$V = \frac{1}{n}(R^{\frac{2}{3}}S^{\frac{1}{2}})$ or $Q = \frac{1}{n}(AR^{\frac{2}{3}}S^{\frac{1}{2}})$

where:
Q = flow rate
V = velocity
n = index of roughness known as "Manning's n"
R= hydraulic radius (cross-section area divided by wetted perimeter)
A = cross sectional area
S = slope of the channel

Additionally, the areas of each cross-section were computed by dividing it into sub-sections. The average width per sub-section was taken by using the formula:

$\overline{w} = \frac{(w_1+\frac{w_2}{2})^2}{2W_1}$ (For the First & Last Section)
$\overline{w} = (\frac{w_i}{2} + \frac{w_{i+1}}{2})$ (For the Rest of the Segments)

Moreover, the average width of each subsection was then multiplied to their depth to get their corresponding area. The total area of the cross-section was taken by adding all the areas of its sub-sections. The computed peak discharge is shown in table.

Table.2. Computed Peak Discharge

Subbasin	Station	Computed Peak Discharge (m^3/s)
Subbasin-4	531.9539	1129.9
Subbasin-5	1551.457	154.2
Subbasin-6	4285.935	163.4
	2120.811	769.7
	916.8855	261.6

To determine whether there is flooding or not, the computed maximum discharge capacities were compared with the simulated peak discharges based on every year return period given.

III. Results and Discussion

For a variety of hydrological simulations, HEC-HMS models are reliable. The HEC-HMS model was run to simulate 2-, 5-, 10-, 15-, 20-, 25-, 50- and 100-year return period to determine the peak discharge in m3/s. Moreover, HEC-RAS was used to view and compute the capacity of the cross-section of the river network of each subbasin.

3.1 Peak discharge with 2-Year Return Period

Based on the 2-year return period, the calculated peak discharge on Sink 1 to Sink 4 of the watershed was 457.3 m^3/s, 268.2 m^3/s, 53 m^3/s, and 87.5 m^3/s respectively. The flood hydrograph at the watershed's sinks with a 2-year return period is presented in Figure 4.

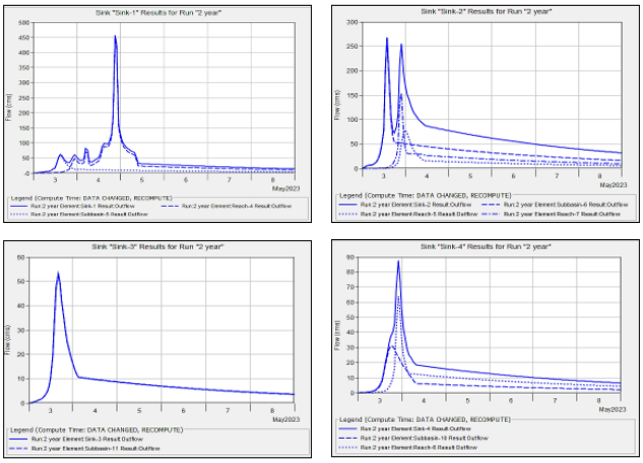

Fig.4.Flood Hydrograph of the Watershed based on 2-Year Return Period

As shown in Table 3, the computed peak discharges were compared with the simulated 2- year design storm peak discharges to determine the occurrence of flooding. The computed peak discharge for Subbasin 4 stationed at 531.9539 was less than simulated peak discharge, thus there is no flooding. For Subbasin 5 stationed at 1551.457, the computed peak discharge was also less than the simulated peak discharges, thus there is no flooding. Moreover, for Subbasin 6 stationed at 4285.935, 2120.811 and 916.8855, the computed peak discharges were also less than the simulated peak discharges, thus there is also no flooding.

Table.3. Computed Peak Discharge vs. the 2-Year Simulated Peak Discharge

2-YEAR SIMULATION RUN					
Subbasin	Station	Cross-Section (HEC-RAS)	Computed Peak Discharge (m^3/s)	Simulated Peak Discharge (m^3/s)	Flooding
Subbasin-4	531.9539	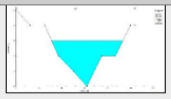	70.999	44.2	No Flooding
Subbasin-5	1551.457	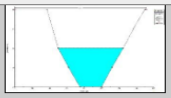	105.691	59.3	No Flooding
Subbasin-6	4285.935	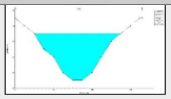	512.71	266.3	No Flooding
	2120.811	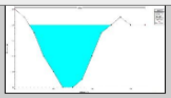	466.125	266.3	No Flooding
	916.8855	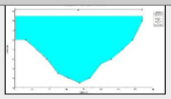	478.251	266.3	No Flooding

Note: *Due to insufficient data, the cross-sections were limited only to the available cut lines with cross-sections that are well-defined and with areas that can be solved through manual computations.*

3.2 Peak discharge with 5-Year Return Period

Based on the 5-year return period, the calculated peak discharge on Sink 1 to Sink 4 of the watershed was 674.2 m^3/s, 411.7 m^3/s, 83 m^3/s, and 138.0 m^3/s respectively. The flood hydrograph at the watershed's sinks with a 5-year return period is presented in Figure 5.

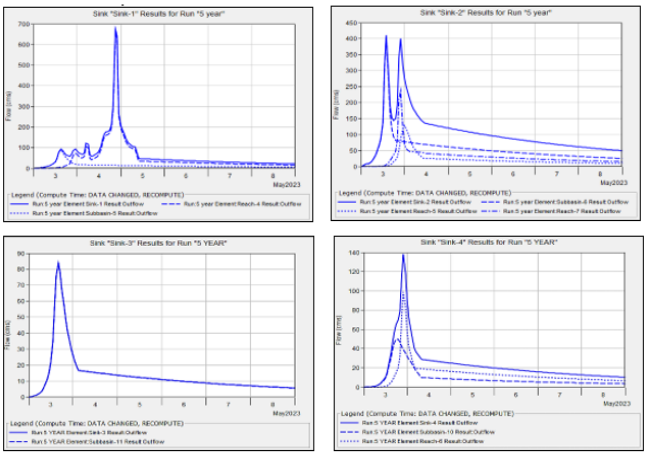

Fig.5. Flood Hydrograph of the Watershed based on 5-Year Return Period

As shown in Table 4, the computed peak discharges were compared with the simulated 5-year design storm peak discharges to determine the occurrence of flooding. The computed peak discharge for Subbasin 4 stationed at 531.9539 was less than simulated peak discharge, thus there is no flooding. For Subbasin 5 stationed at 1551.457, the computed peak discharge was also less than the simulated peak discharges, thus there is no flooding. Moreover, for Subbasin 6 stationed at 4285.935, 2120.811 and 916.8855, the computed peak discharges were also less than the simulated peak discharges, thus there is also no flooding.

Table.4. Computed Peak Discharge vs. the 5-Year Simulated Peak Discharge

5-YEAR SIMULATION RUN					
Subbasin	Station	Cross-Section (HEC-RAS)	Computed Peak Discharge (m^3/s)	Simulated Peak Discharge (m^3/s)	Flooded
Subbasin-4	531.9539	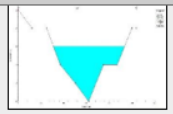	70.999	66.3	No Flooding
Subbasin-5	1551.457	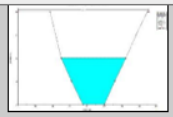	512.71	87.5	No Flooding
Subbasin-6	4285.935	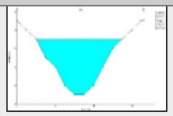	622.340	404.4	No Flooding
	2120.811	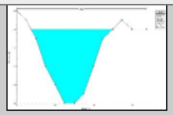	466.125	404.4	No Flooding
	916.8855	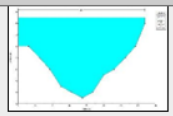	478.251	404.4	No Flooding

Note: *Due to insufficient data, the cross-sections were limited only to the available cut lines with cross-sections that are well-defined and with areas that can be solved through manual computations.*

3.3 Peak discharge with 10-Year Return Period

Based on the 10-year return period, the calculated peak discharge on Sink 1 to Sink 4 of the watershed was 814.7 m^3/s, 506.5 m^3/s, 103.8 m^3/s, and 171.0 m^3/s respectively. The flood hydrograph at the watershed's sinks with a 10-year return period is presented in Figure 6.

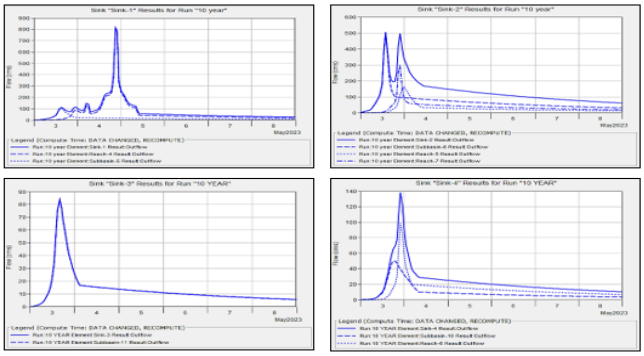

Fig.6. Flood Hydrograph of the Watershed based on 10-Year Return Period

As shown in Table 5, the computed peak discharges were compared with the simulated 10-year design storm peak discharges to determine the occurrence of flooding. The computed peak discharge for Subbasin 4 stationed at 531.9539 was greater than simulated peak discharge, thus there is flooding. For Subbasin 5 stationed at 1551.457, the computed peak discharge was also greater than the simulated peak discharges, thus there is also flooding. Meanwhile, for Subbasin 6 stationed at 4285.935, the computed peak discharge was less than the simulated peak discharges, thus there is no flooding. Lastly, for Subbasin 6 stationed at 2120.811 and 916.8855, the computed peak discharges were greater than the simulated peak discharges, thus there is flooding.

Table.5. Computed Peak Discharge vs. the 10-Year Simulated Peak Discharge

10-YEAR SIMULATION RUN					
Subbasin	Station	Cross-Section (HEC-RAS)	Computed Peak Discharge (m^3/s)	Simulated Peak Discharge (m^3/s)	Flooded
Subbasin-4	531.9539	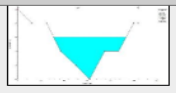	70.999	80.7	Flooding
Subbasin-5	1551.457	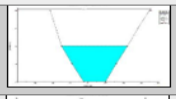	105.691	106.0	Flooding
Subbasin-6	4285.935	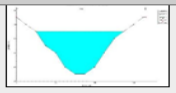	512.71	494.1	No Flooding
	2120.811	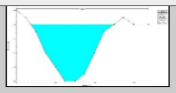	466.125	494.1	Flooding
	916.8855	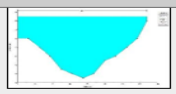	478.251	494.1	Flooding

Note: *Due to insufficient data, the cross-sections were limited only to the available cut lines with cross-sections that are well-defined and with areas that can be solved through manual computations.*

3.4 Peak discharge with 15-Year Return Period

Based on the 15-year return period, the calculated peak discharge on Sink 1 to Sink 4 of the watershed was 892.7 m^3/s, 560.0 m^3/s, 115.1 m^3/s, and 189.5 m^3/s respectively. The flood hydrograph at the watershed's sinks with a 15-year return period is presented in Figure 7.

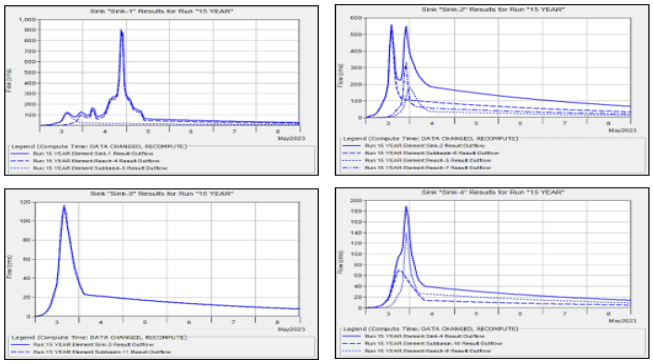

Fig.7. Flood Hydrograph of the Watershed based on 15-Year Return Period

As shown in Table 6, the computed peak discharges were compared with the simulated 15-year design storm peak discharges to determine the occurrence of flooding. The computed peak discharge for Subbasin 4 stationed at 531.9539 was greater than simulated peak discharge, thus there is flooding.

Table.6. Computed Peak Discharge vs. the 15-Year Simulated Peak Discharge

15-YEAR SIMULATION RUN					
Subbasin	Station	Cross-Section (HEC-RAS)	Computed Peak Discharge (m^3/s)	Simulated Peak Discharge (m^3/s)	Flooded
Subbasin-4	531.9539	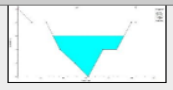	70.999	88.8	Flooding
Subbasin-5	1551.457	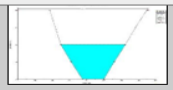	105.691	116.4	Flooding
Subbasin-6	4285.935	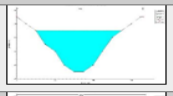	512.71	544.3	Flooding
	2120.811	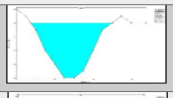	466.125	544.3	Flooding
	916.8855	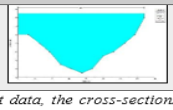	478.251	544.3	Flooding

Note: *Due to insufficient data, the cross-sections were limited only to the available cut lines with cross-sections that are well-defined and with areas that can be solved through manual computations.*

For Subbasin 5 stationed at 1551.457, the computed peak discharge was also greater than the simulated peak discharges, thus there is also flooding.

Moreover, for Subbasin 6 stationed at 4285.935, 2120.811 and 916.8855, the computed peak discharges were also greater than the simulated peak discharges, thus there is also flooding.

3.5 Peak discharge with 20-Year Return Period

Based on the 20-year return period, the calculated peak discharge on Sink 1 to Sink 4 of the watershed was 947.4 m^3/s, 597.3 m^3/s, 123.0 m^3/s, and 202.3 m^3/s respectively. The flood hydrograph at the watershed's sinks with a 20-year return period is presented in Figure 8.

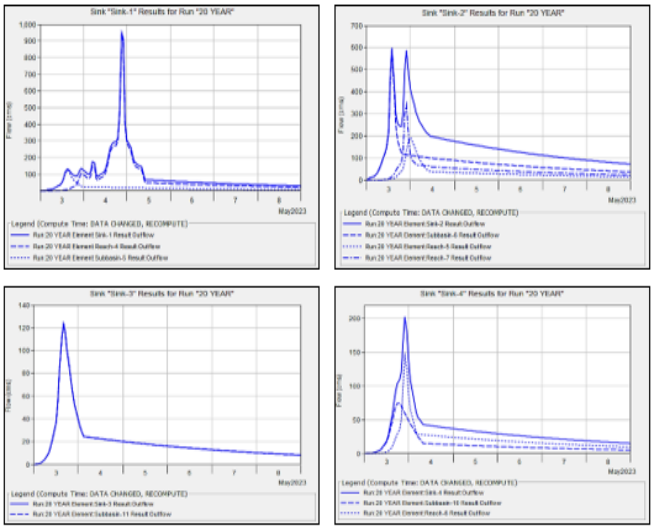

Fig.8. Flood Hydrograph of the Watershed based on 20-Year Return Period

As shown in Table 7, the computed peak discharges were compared with the simulated 20-year design storm peak discharges to determine the occurrence of flooding. The computed peak discharge for Subbasin 4 stationed at 531.9539 was greater than simulated peak discharge, thus there is flooding.

For Subbasin 5 stationed at 1551.457, the computed peak discharge was also greater than the simulated peak discharges, thus there is also flooding. Moreover, for Subbasin 6 stationed at 4285.935, 2120.811 and 916.8855, the computed peak discharges were also greater than the simulated peak discharges, thus there is also flooding.

Table.7. Computed Peak Discharge vs. the 20-Year Simulated Peak Discharge

20-YEAR SIMULATION RUN					
Subbasin	**Station**	**Cross-Section (HEC-RAS)**	**Computed Peak Discharge (m^3/s)**	**Simulated Peak Discharge (m^3/s)**	**Flooded**
Subbasin-4	531.9539	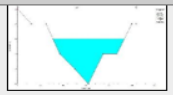	70.999	94.5	Flooding
Subbasin-5	1551.457	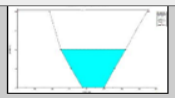	105.691	123.7	Flooding
Subbasin-6	4285.935	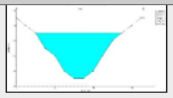	512.71	579.1	Flooding
	2120.811	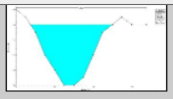	466.125	579.1	Flooding
	916.8855	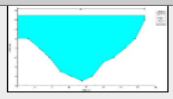	478.251	579.1	Flooding

***Note**: Due to insufficient data, the cross-sections were limited only to the available cut lines with cross-sections that are well-defined and with areas that can be solved through manual computations.*

3.6 Peak discharge with 25-Year Return Period

Based on the 25-year return period, the calculated peak discharge on Sink 1 to Sink 4 of the watershed was 989.5 m^3/s, 629.0 m^3/s, 129.1 m^3/s, and 212.2 m^3/s respectively. The flood hydrograph at the watershed's sinks with a 25-year return period is presented in Figure 9.

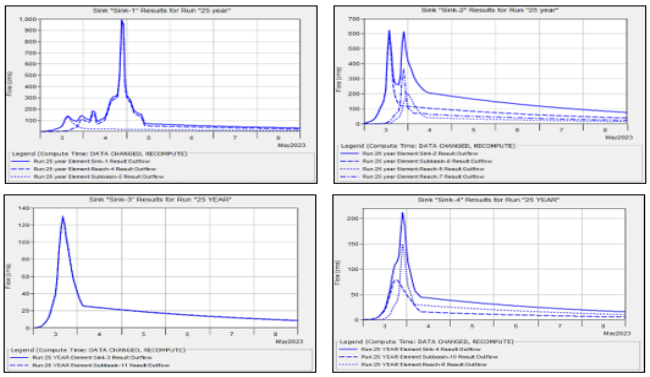

Fig.9. Computed Peak Discharge vs. the 25-Year Simulated Peak Discharge

As shown in Table 19, the computed peak discharges were compared with the simulated 25-year design storm peak discharges to determine the occurrence of flooding. The computed peak discharge for Subbasin 4 stationed at 531.9539

was greater than simulated peak discharge, thus there is flooding. For Subbasin 5 stationed at 1551.457, the computed peak discharge was also greater than the simulated peak discharges, thus there is also flooding. Moreover, for Subbasin 6 stationed at 4285.935, 2120.811 and 916.8855, the computed peak discharges were also greater than the simulated peak discharges, thus there is also flooding.

Table.8. Computed Peak Discharge vs. the 25-Year Simulated Peak Discharge

25-YEAR SIMULATION RUN					
Subbasin	Station	Cross-Section (HEC-RAS)	Computed Peak Discharge (m^3/s)	Simulated Peak Discharge (m^3/s)	Flooded
Subbasin-4	531.9539	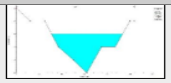	70.999	98.8	Flooding
Subbasin-5	1551.457	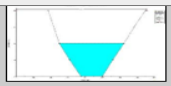	105.691	129.2	Flooding
Subbasin-6	4285.935	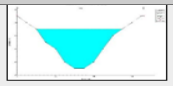	512.71	605.8	Flooding
	2120.811	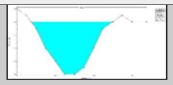	466.125	605.8	Flooding
	916.8855	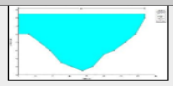	478.251	605.8	Flooding

Note: *Due to insufficient data, the cross-sections were limited only to the available cut lines with cross-sections that are well-defined and with areas that can be solved through manual computations.*

3.7 Peak discharge with 50-Year Return Period

Based on the 50-year return period, the calculated peak discharge on Sink 1 to Sink 4 of the watershed was 1117.6 m^3/s, 715.1 m^3/s, 147.9 m^3/s, and 242. 7 m^3/s respectively. The flood hydrograph at the watershed's sinks with a 50-year return period is presented in Figure 10.

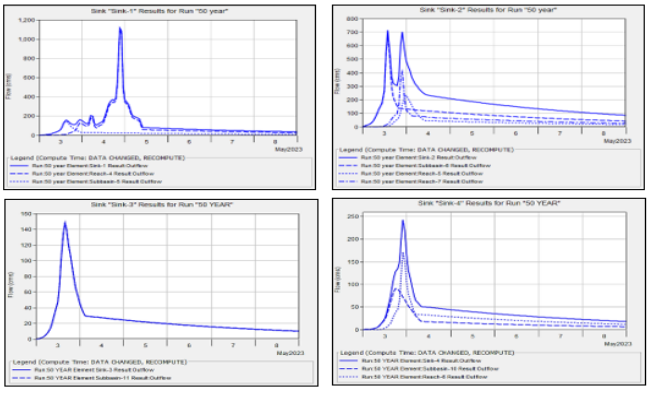

Fig.10. Computed Peak Discharge vs. the 50-Year Simulated Peak Discharge

As shown in Table 9, the computed peak discharges were compared with the simulated 25-year design storm peak discharges to determine the occurrence of flooding. The computed peak discharge for Subbasin 4 stationed at 531.9539 was greater than simulated peak discharge, thus there is flooding. For Subbasin 5 stationed at 1551.457, the computed peak discharge was also greater than the simulated peak discharges, thus there is also flooding. Moreover, for Subbasin 6 stationed at 4285.935, 2120.811 and 916.8855, the computed peak discharges were also greater than the simulated peak discharges, thus there is also flooding.

Table.9.Computed Peak Discharge vs. the 50-Year Simulated Peak Discharge

50-YEAR SIMULATION RUN					
Subbasin	Station	Cross-Section (HEC-RAS)	Computed Peak Discharge (m^3/s)	Simulated Peak Discharge (m^3/s)	Flooded
Subbasin-4	531.9539	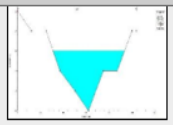	70.999	112.2	Flooding
Subbasin-5	1551.457	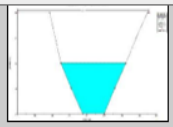	105.691	146.4	Flooding
Subbasin-6	4285.935	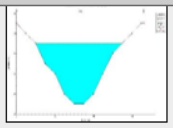	512.71	668.5	Flooding
	2120.811	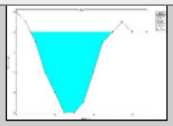	466.125	668.5	Flooding
	916.8855	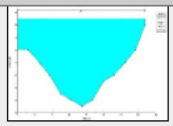	478.251	668.5	Flooding

Note: *Due to insufficient data, the cross-sections were limited only to the available cut lines with cross-sections that are well-defined and with areas that can be solved through manual computations.*

3.8 Peak discharge with 100-Year Return Period

Based on the 100-year return period, the calculated peak discharge on Sink 1 to Sink 4 of the watershed was 1244.8 m^3/s, 803.1 m^3/s, 166.3 m^3/s, and 272.7 m^3/s respectively. The flood hydrograph at the watershed's sinks with a 100-year return period is presented in Figure 11.

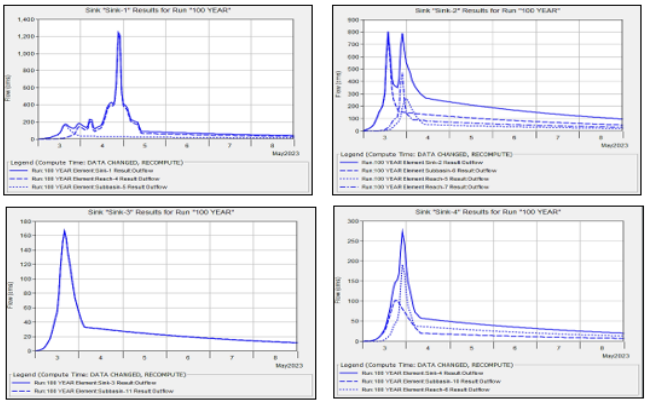

Fig.11. Computed Peak Discharge vs. the 100-Year Simulated Peak Discharge

As shown in Table 10, the computed peak discharges were compared with the simulated 50-year design storm peak discharges to determine the occurrence of flooding. The computed peak discharge for Subbasin 4 stationed at 531.9539 was greater than simulated peak discharge, thus there is flooding. For Subbasin 5 stationed at 1551.457, the computed peak discharge was also greater than the simulated peak discharges, thus there is also flooding. Moreover, for Subbasin 6 stationed at 4285.935, 2120.811 and 916.8855, the computed peak discharges were also greater than the simulated peak discharges, thus there is also flooding.

Table.10. Computed Peak Discharge vs. the 100-Year Simulated Peak Discharge

100-YEAR SIMULATION RUN					
Subbasin	Station	Cross-Section (HEC-RAS)	Computed Peak Discharge (m^3/s)	Simulated Peak Discharge (m^3/s)	Flooded
Subbasin-4	531.9539	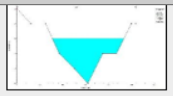	70.999	125.5	Flooding
Subbasin-5	1551.457	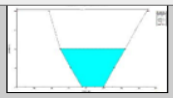	105.691	163.4	Flooding
Subbasin-6	4285.935	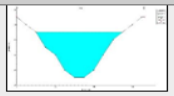	512.71	769.7	Flooding
	2120.811	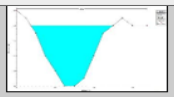	466.125	769.7	Flooding
	916.8855	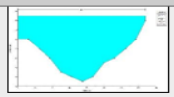	478.251	769.7	Flooding

Note: *Due to insufficient data, the cross-sections were limited only to the available cut lines with cross-sections that are well-defined and with areas that can be solved through manual computations.*

IV. Conclusion and Recommendation

Based on the results, the highest peak discharge for all elements was calculated for the 100-year return period design storm while the lowest was calculated on the 2-year return period. Among the subbasins, the highest peak discharge was generated in Subbasin 1 for all the design storm simulation which also constitutes the largest area among the Subbasin. Meanwhile, lowest peak discharge was generated in Subbasin 10.

Moreover, as revealed on the results, some parts were already flooded in Subbasin 6 by the design storm with a 10-year return period. The Subbasin 6 comprises some parts of barangay San Pedro, San Juan, San Jose, San Nicolas, Sta. Cruz and San Miguel.

Meanwhile, for the succeeding year return periods, namely 10-, 15-, 20-, 25-, 50- and 100-year return periods, selected stations from Subbasin, 4, 5 and 6 were all flooded. Subbasin 4 comprises some parts of barangay San Pablo Libutad and Dela Paz. Meanwhile, subbasin 5 comprises some parts of barangay Dela Paz, San Pablo Libutad, San Pablo Proper, San Isidro, San Pedro and Sta. Monica.

Floods can be mitigated through more than just structural development. The simulation of peak discharge data generated in this study can be utilized for flood management. Moreover, the data generated from this study can also be used to lower the danger of flooding through hydraulic modeling and mapping the flood inundation zones.

Limitation in acquired data has limited some methods that were used in the study. The proponents of this study recommend future researchers to explore other methods in modeling using HEC-HMS once more data were made available.

Moreover, because of the lack of resources to obtain a more accurate DEM, the selected cross-sections were only limited to those with well-defined cross sections and those with areas that can be computed theoretically through manual computations. The researchers recommend further studies once an updated and more accurate DEM was made accessible.

References

[1]. Adnan, R., Abd M. S., & Fazlina A.R. (2016). A 3-hours river water level flood prediction model using NNARX with improves modelling strategy. 23–27.

[2]. Alaghmand, S., bin Abdullah, R., Abustan, I., & Eslamian, S. (2012). Comparison between capabilities of HEC-RAS and MIKE11 hydraulic models in river flood risk modeling (a case study of Sungai Kayu Ara River basin, Malaysia).

International Journal of Hydrology Science and Technology, 2(3), 270–291.

[3]. Balvanshi, A., & Tiwari, H. L. (2019). A Comprehensive Review of Runoff Estimation by the Curve Number Method.

[4]. Barnes, T. S., Alvaran, P. J. J., Lantican, T. L. D. C., Lapuz, E. L., Ignacio, C., Baluyut, A. S., Parke, C. R., Palaniappan, G., Cameron, D., Ancog, R. C., Mananggit, M. R., de Castro, R., Meers, J., Palmieri, C., Turni, C., Villar, E. C., & Blackall, P. J. (2020). Combining conventional and participatory approaches to identify and prioritise management and health-related constraints to smallholder pig production in San Simon, Pampanga, Philippines. Preventive Veterinary Medicine, 178, 104987.

[5]. Bricker, J., Takagi, H., Mas, E., Kure, S., Adriano, B., Yi, C., & Roeber, V. (2014). Spatial variation of damage due to storm surge and waves during typhoon Haiyan in the Philippines. Journal of Japan Society of Civil Engineers, 70(2), 231–235.

[6]. Callanga, C., Alegrado, C. A., Hurano, K., Tenio, G. S., Velarde, P., Maristela, C., & Galon, V. (2020). River water lever sensor as river flood warning system. International Journal of Physical Sciences Full Length Research Paper, 15(4), 138–150.

[7]. Clasing, R., & Muñoz, E. (2018). Estimating the Optimal Velocity Measurement Time in Rivers' Flow Measurements: An Uncertainty Approach. Water 2018, Vol. 10, Page 1010, 10(8), 1010.

[8]. Faruq, A., Marto, A., Izzaty, N. K., Kuye, A. T., Mohd Hussein, S. F., & Abdullah, S. S. (2021). Flood Disaster and Early Warning: Application of ANFIS for River Water Level Forecasting. Kinetik: Game Technology, Information System, Computer Network, Computing, Electronics, and Control, 1–10.

[9]. Garcia, M., Hernandez, I., Hernandez, J., & Tovar, R. (2015). Roughness Manning Coefficient Variation in Irrigation Open Channels by Changing Width and Roughness Surface in the Armfield C4MKII Equipment. American Society of Agricultural and Biological Engineers.

[10]. Gichamo, T. Z., Popescu, I., Jonoski, A., & Solomatine, D. (2012). River cross-section extraction from the ASTER global DEM for flood modeling. Environmental Modelling & Software, 31, 37–46.

[11]. Hadi, Z. N., & Almansori, N. J. H. (2023). Estimation of Manning coefficient for the section between Al-Hindiya barrage and Al-Kufa barrage utilizing HEC-RAS. Materials Today: Proceedings, 80, 2595–2601.

[12]. Halwatura, D., & Najim, M. M. M. (2013). Application of the HEC-HMS model for runoff simulation in a tropical catchment. Environmental Modelling & Software, 46, 155–162.

[13]. Introduction to HEC-RAS. (n.d.). Retrieved June 14, 2023.

[14]. Irrigation Engineering: LESSON 5 Methods of Water Measurements in Open Channels. (n.d.). Retrieved June 14, 2023.

[15]. M. S. H. Mondal, T. Murayama and S. Nishikizawa, "Assessing the flood risk of riverine households: A case study from the right bank of the Teesta River, Bangladesh," International Journal of Disaster Risk Reduction, vol. 51, pp. 101758, 2020.

[16]. Nagumo, N., & Sawano, H. (2016). Land Classification and Flood Characteristics of the Pampanga River Basin, Central Luzon, Philippines. Journal of Geography (Chigaku Zasshi), 125(5), 699–716.

[17]. Puno, G. R., Marin, R. A., Angelica Amper, R. L., & Allan Talisay, B. M. (2018). Flood simulation using geospatial models in Manupali Flood simulation using geospatial and hydrologic models in Manupali Watershed, Bukidnon, Philippines. Philippines Article in Journal of Biodiversity and Environmental Sciences, 294(3), 294–303.

[18]. Santillan, J. R., Marqueso, J. T., Makinano-Santillan, M., & Serviano, J. L. (2016). Beyond flood hazard maps: Detailed flood characterization with remote sensing, gis and 2D modelling. International Archives of the Photogrammetry, Remote Sensing and Spatial Information Sciences - ISPRS Archives, 42(4W1), 315–323.

[19]. Sulistyowati, R., Sujono, H. A., & Musthofa, A. K. (2016). A river water level monitoring system using android-based wireless sensor networks for a flood early warning system. Lecture Notes in Electrical Engineering, 365, 401–408.

[20]. Tabios III, G. Q. (2020). Water Resources Systems of the Philippines: Modeling Studies. 4.

[21]. Toda, L. L., Yokingco, J. C. E., Paringit, E. C., & Lasco, R. D. (2017). A LiDAR-based flood modelling approach for mapping rice cultivation areas in Apalit, Pampanga. Applied Geography, 80, 34–47.